



# Woody species do not differ in dormancy progression: Differences in time to budbreak due to forcing and cold hardiness

Al P. Kovaleski<sup>a,b,1</sup>

Edited by Pamela Soltis, University of Florida, Gainesville, FL; received July 2, 2021; accepted March 29, 2022

Budbreak is one of the most observed and studied phenological phases in perennial plants, but predictions remain a challenge, largely due to our poor understanding of dormancy. Two dimensions of exposure to temperature are generally used to model budbreak: accumulation of time spent at low temperatures (chilling) and accumulation of heat units (forcing). These two effects have a well-established negative correlation; with more chilling, less forcing is required for budbreak. Furthermore, temperate plant species are assumed to vary in chilling requirements for dormancy completion allowing proper budbreak. Here, dormancy is investigated from the cold hardiness standpoint across many species, demonstrating that it should be accounted for to study dormancy and accurately predict budbreak. Most cold hardiness is lost prior to budbreak, but rates of cold hardiness loss (deacclimation) vary among species, leading to different times to budbreak. Within a species, deacclimation rate increases with accumulation of chill. When inherent differences between species in deacclimation rate are accounted for by normalizing rates throughout winter by the maximum rate observed, a standardized deacclimation potential is produced. Deacclimation potential is a quantitative measurement of dormancy progression based on responsiveness to forcing as chill accumulates, which increases similarly for all species, contradicting estimations of dormancy transition based on budbreak assays. This finding indicates that comparisons of physiologic and genetic control of dormancy require an understanding of cold hardiness dynamics. Thus, an updated framework for studying dormancy and its effects on spring phenology is suggested where cold hardiness in lieu of (or in addition to) budbreak is used.

dormancy | spring phenology | cold hardiness | budbreak | climate change

Spring phenology defines the long-term survival and fitness of perennial plants within environments with below-freezing winter temperatures (1, 2). Spring kills of breaking buds by low temperature are widely regarded as a major aspect influencing species distribution (3), and risks associated with it have shifted (mostly increased) due to climatic changes (4–8), making accurate predictions key to understanding adaptation to future climates (9). Yet, accurate predictions remain a major challenge (10, 11), and climate change may create environmental conditions in colder climates that are not analogous to those in presently warmer regions (i.e., climates are not only moving up in latitude) (12). Artificial warming experiments have been used in order to study possible future conditions (13, 14), but results from these experiments do not match observations of advanced budbreak over the last few decades of climate warming (10). This mismatch demonstrates that we still lack a fundamental understanding of the budbreak process, and thus, empirical studies are required to understand the environmental effects that define the time to budbreak in woody species (11).

Considerable prior research has attempted to predict the effects of climate change on phenology (3, 10, 15–31). For spring phenology, temperature is generally agreed to be the largest contributing factor (21, 26, 28, 32), and studies focus on interactions between chilling (accumulation of time spent in low temperatures) and forcing (accumulation of thermal time, growing degree days [GDD]) as temperature effects on budbreak, with reference to shifts in their interaction in a changing climate (10, 15, 21, 33). Other factors have also been studied for their effects on budbreak, such as wood porosity (34), nutritional status (35), water availability (36, 37)—including humidity (38)—and especially, photoperiod (39, 40) [be that through more radiative warming (41) or true light-quality effects (42–44)]. However, a missing key component of winter survival, the dynamic and changing cold hardiness of buds, has remained unexplored as the starting point for the estimation of the time to achieve any phenological stage. The pattern of cold hardiness of buds is U shaped, where it increases during fall (acclimation), is maintained during winter, and is lost during spring (deacclimation)—all

## Significance

Better knowledge of dormancy (plant “hibernation”) is required to understand future adaptation of woody perennial plants facing warmer climates. Typical dormancy research uses time to budbreak to define the transition from a warm temperature nonresponsive to a responsive state (long vs. short time to budbreak). Based on this phenotyping method, species diverge in dormancy transition times during winter. Here, dynamics of bud cold hardiness (lowest survival temperature) for many species are used to show convergence in their response to winter chilling. Therefore, previous studies determining chilling requirement based on budbreak may describe adaptation to an environment but do not accurately describe physiological dormancy transitions. Further, cold hardiness dynamics can be used for field predictions of bud cold hardiness and budbreak.

Author affiliations: <sup>a</sup>Department of Horticulture, University of Wisconsin–Madison, Madison, WI 53706; and <sup>b</sup>Arnold Arboretum of Harvard University, Boston, MA 02131

Author contributions: A.P.K. designed research, performed research, analyzed data, and wrote the paper.

The author declares no competing interest.

This article is a PNAS Direct Submission.

Copyright © 2022 the Author(s). Published by PNAS. This article is distributed under [Creative Commons Attribution-NonCommercial-NoDerivatives License 4.0 \(CC BY-NC-ND\)](https://creativecommons.org/licenses/by-nc-nd/4.0/).

<sup>1</sup>Email: al.kovaleski@wisc.edu.

This article contains supporting information online at <http://www.pnas.org/lookup/suppl/doi:10.1073/pnas.2112250119/-/DCSupplemental>.

Published May 2, 2022.

largely in response to air temperature and differing by species. Most phenological models fail to account for these species-specific differences in bud cold hardiness, at all times during the dormant season, and in any location or climate, despite existing empirical evidence that artificial acclimation increases time to budbreak (45). It is also widely known that species have different temperature thresholds for tissue damage during bud swell, budbreak, and leaf out (9, 22), as well as in midwinter (22, 45, 46). This suggests that the amount of cold hardiness buds need to lose to transition from their cold hardy state to budbreak (the deacclimation path length in degrees Celsius) differs among species and climates and throughout the dormant season. Despite information existing on these cold hardiness effects on budbreak (45, 47), the influence of cold hardiness has remained largely unexplored on the prediction of field budbreak.

Another and possibly most critical source of uncertainty in predictions of phenology is our poor understanding of dormancy. Time spent in low temperatures (chilling) has been long known to promote the transition from a dormancy phase that is nonresponsive to growth-conducive temperatures (i.e., endodormancy, rest) to a responsive phase (ecodormancy, quiescence) (48). Some species, or genotypes within species, are thought to have lower chilling requirements than others based on faster budbreak in forcing conditions (e.g., 22 °C and 16-h day length). This observation results in comparative classifications of “low–chill requirement” and “high–chill requirement” plants. However, there are still questions about the temperature range where chilling that promotes the bud dormancy transition occurs and how much chilling they provide (49, 50), leading to multiple methods for estimation of chill accumulation (51–55) without a full comprehension of the mechanism or pathway for dormancy and in turn, a low ability in predicting budbreak. This is despite a growing list of dormancy-related genes and chemicals that promote dormancy transitions (56–61).

Recent work has shown that rates of cold hardiness loss (deacclimation) increase with chilling accumulation, which can be used to study dormancy progression (47). By standardizing the rates to the maximum observed rate at the end of the dormant season, this measurement is referred to as deacclimation potential ( $\Psi_{deacc}$ ), which varies from zero to one [or 0 to 100% (47)]. The  $\Psi_{deacc}$  is the increase in responsiveness to forcing observed as chill accumulates, and it is a quantitative measurement of dormancy. In analogous terms,  $\Psi_{deacc} = 0$  would mean entirely endodormant buds (nontemperature-responsive buds), and  $\Psi_{deacc} = 1$  would mean entirely ecodormant buds (maximum temperature responsiveness), acknowledging a quantitative progress in dormancy rather than a qualitative transition.

Three sources of variation in time to budbreak are thus investigated in the present study: the initial cold hardiness of buds collected for a given assay (the departure point,  $CH_0$ ), the cold hardiness at budbreak ( $CH_{BB}$ ), and the effective rate of cold hardiness loss (deacclimation;  $k_{deacc}^*$ ). The relationship of these variables is used here as

$$\text{Time to Budbreak} = \frac{|CH_0 - CH_{BB}|}{k_{deacc}^*}, \quad [1]$$

where  $|CH_0 - CH_{BB}|$  defines the path length in degrees Celsius from the cold hardy state to budbreak. An example of this relationship is shown in Fig. 1; two rates of deacclimation, 4 °C d<sup>-1</sup> and 1 °C d<sup>-1</sup>, are given for a common path length of 20 °C. These two deacclimation rates result in 5 and 20 d to budbreak, respectively. In the context presented here, the differences in rates of deacclimation can be due to different levels of chilling accumulation (modulation of the deacclimation rate by  $\Psi_{deacc}$ ), leading to

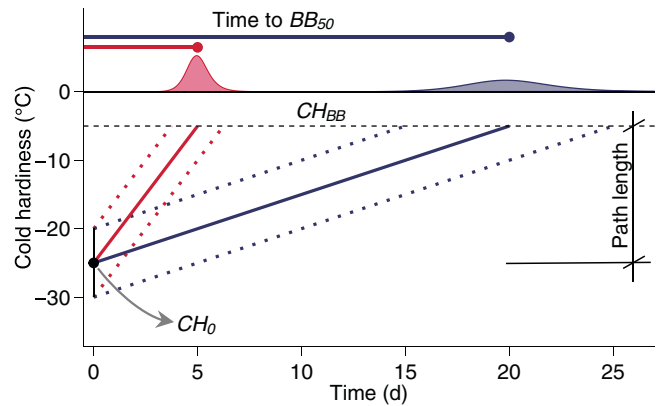


**Fig. 1.** Sources of variation in time to budbreak. The initial cold hardiness ( $CH_0$ ) is that of buds collected from the field. In order to reach budbreak, buds must lose their initial cold hardiness and reach the cold hardiness at budbreak ( $CH_{BB}$ ). This distance from  $CH_0$  to  $CH_{BB}$  is the path length (in degrees Celsius). For the same path length, time of budbreak is then defined by how fast the path is traveled: the effective rate of deacclimation ( $k_{deacc}^*$ ; the slopes of the two lines). A higher rate of deacclimation (red line) leads to concentrated and earlier budbreak, whereas a lower rate (blue line) means budbreak occurs later and more sporadically (density curves).

apparent differences in forcing requirement. Alternatively, these may represent species with different rates of deacclimation at the same level of chilling accumulation. This relationship (Eq. 1) demonstrates the effect of path length on time to budbreak; if the path length increased by 5 °C for both to a total of 25 °C (e.g., buds of the same two species but from a region with lower minimum temperatures causing a lower  $CH_0$ ), time to budbreak would increase by 1 and 5 d, respectively, at the same rates of deacclimation (hypothetical scenarios are presented more extensively in *SI Appendix*, *SI Text* and Figs. S1–S6). In natural conditions, it is expected that species will vary in each of these three aspects: levels of cold hardiness throughout the winter, cold hardiness at which budbreak is displayed, and rates of deacclimation. Because timing of budbreak is affected by chill accumulation and spring temperatures, the hypothesis is that rates of deacclimation will also be affected by both chill accumulation and ambient spring temperature within the same species.

The objective of this study was to determine how temperature and chill accumulation affects deacclimation and how this in turn affects budbreak in multiple species. To study these effects, over 40,500 cold hardiness measurements and 8,000 cuttings for budbreak observation from 15 species collected over two dormant seasons were used as proxy for whole-plant responses (62). The 15 species represent both gymnosperms and angiosperms, deciduous and evergreen, nine families (Cornaceae, Cupressaceae, Ericaceae, Fabaceae, Fagaceae, Oleaceae, Pinaceae, Rosaceae, and Sapindaceae), three continents and many climates of origin, of horticultural and ecological importance, with both regular and naked buds, and they are planted at the Arnold Arboretum of Harvard University located in Boston, MA (Fig. 2). The phenotype that unites all species studied is that all have buds that survive low temperatures by promoting supercooling of water (63). In general, four species are presented in the main figures as examples for the concepts (*Abies balsamea*, *Cercis canadensis*, *Forsythia* × ‘Meadowlark,’ and *Larix kaempferi*), but results for all species are presented in *SI Appendix*.

## Results

The species studied differed in their cold hardiness determined weekly throughout the winter (Fig. 3 and *SI Appendix*, Fig. S7).

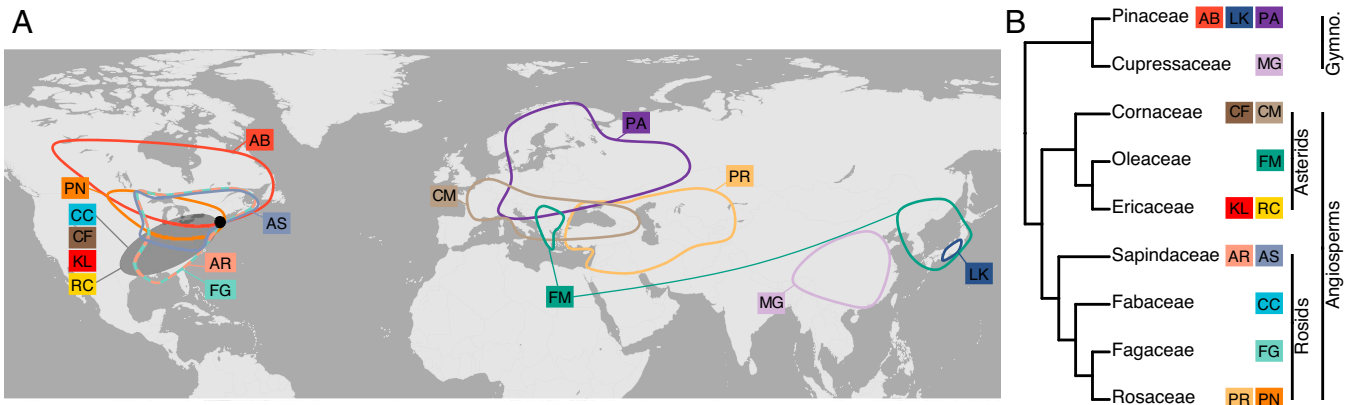


**Fig. 2.** Distribution and relatedness of species studied. (A) Approximate native distribution of the 15 species studied, which are distributed in three continents and have different latitudes of origin. *Forsythia* × 'Meadowlark' (FM) is an interspecific hybrid. The black point indicates the location of the Arnold Arboretum of Harvard University. (B) A cladogram shows the relatedness of the species studied at the family level. AB, *A. balsamea*; AR, *A. rubrum*; AS, *A. saccharum*; CC, *C. canadensis*; CF, *C. florida*; CM, *C. mas*; FG, *F. grandifolia*; KL, *K. latifolia*; LK, *L. kaempferi*; MG, *M. glyptostroboides*; PA, *P. abies*; PN, *P. nigra*; PR, *P. armeniaca*; RC, *R. calendulaceum*.

However, the same general pattern is observed for all species; cold hardiness is gained in the fall, maintained during the winter, and lost before field budbreak in the spring. This response generally follows air temperature (*SI Appendix, Figs. S8 and S9*). For every date of cold hardiness determination, buds were also placed in a growth chamber at 22 °C to observe time to budbreak. Similar patterns were observed across species in terms of time to budbreak (Fig. 3 and *SI Appendix, Fig. S10*). Under forcing, buds take a long time and show a large variability to break when collected in the fall. With the progression of winter, the reverse occurs, with time to budbreak decreasing exponentially and with lower variability.

**Effect of Chill Accumulation (Dormancy) on Rates of Deacclimation.** Weekly field collections were also used to monitor the loss of bud cold hardiness under constant temperature. These buds were in the same growth chamber as those where budbreak was evaluated (22 °C). From these data, effective rates of deacclimation ( $k_{deacc_{22^{\circ}C}}^*$ ) were determined for each collection in degrees Celsius of cold hardiness lost per day (e.g., the slope of the linear regressions is in Fig. 4A; adjusted  $r^2 = 0.79$ ,  $F_{1588,30425} = 76.8$ ,  $P < 0.001$  for all species in all collections combined [individual fits are provided in *SI Appendix*]). The  $k_{deacc_{22^{\circ}C}}^*$  increased with chill accumulation during winter for all species (Fig. 5A and *SI Appendix, Fig. S11*). Based on deacclimation and budbreak

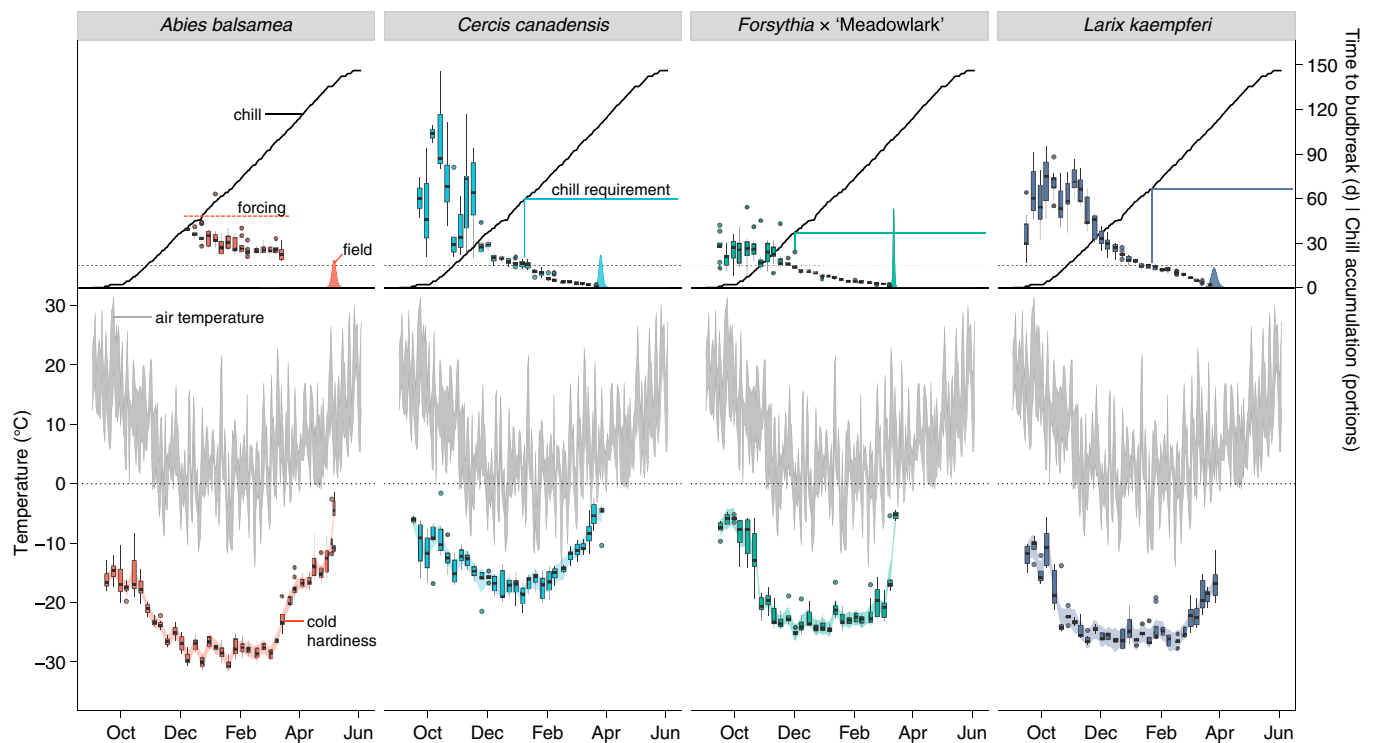


**Fig. 3.** Cold hardiness and time to budbreak relative to air temperature and chill. Cold hardiness of buds measured weekly ( $n \approx 10$ ) throughout the 2019 to 2020 dormant season along with air temperature (Lower; left vertical axis). At each collection, time to reach budbreak under forcing ( $n \approx 10$ ) was also measured along with decreases in response to chill accumulation (Upper; right vertical axis). *SI Appendix, Fig. S7* has further details on air temperature and chill accumulation. Density curves represent observed budbreak in the field (*SI Appendix, Fig. S8*). The dashed lines show the 15-d threshold used for chilling requirement determination.

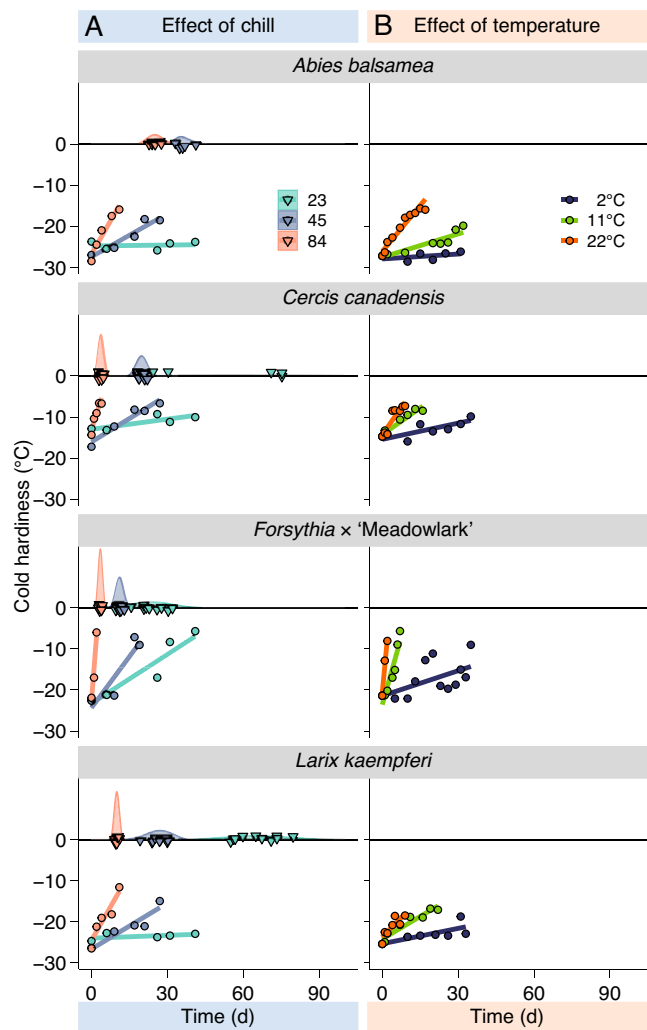


**Fig. 4.** Deacclimation rates and budbreak at different chill accumulations and temperatures. Loss of cold hardness measured (A) at different levels of chill accumulation but the same temperature (22°C) and (B) at different temperatures but same chill accumulation (82 portions). Budbreak was also measured at different levels of chill accumulation (upside down triangles and density curves at the 0°C line in A).

at different chill accumulations, it is notable that budbreak (presented along the 0°C line in Fig. 4A) is linked to the dynamics of deacclimation; lower  $k_{deac_{22^\circ C}}^*$  at 23 chill portions leads to erratic, delayed budbreak, as introduced in Fig. 1. In turn, budbreak occurs much more synchronously with higher  $k_{deac_{22^\circ C}}^*$  at 84 chill portions (i.e., height of the density curves in Fig. 4A). This effect is also observed in species comparisons; at 84 chill portions, buds break earlier and with more uniform timing in *C. canadensis* than in *A. balsamea*.

The maximum rate of deacclimation observed at 22°C ( $\max k_{deac_{22^\circ C}}$ ) differed among species (SI Appendix, Fig. S12). The  $\max k_{deac_{22^\circ C}}$  ranged from 0.6°C d<sup>-1</sup> (*Rhododendron calendulaceum*) to 9.5°C d<sup>-1</sup> (*Forsythia* × ‘Meadowlark’), although the majority of the species tested (11 of 15) exhibited deacclimation rates between 0.5°C d<sup>-1</sup> and 2.0°C d<sup>-1</sup>. Effective rates of deacclimation ( $k_{deac_{22^\circ C}}^*$ ) from each species were then normalized to their corresponding  $\max k_{deac_{22^\circ C}}$ , generating rate proportion measurements or deacclimation potential ( $\Psi_{deacc}$ ) and isolating the effect of chilling accumulation (Fig. 5; SI Appendix, section 4 has further explanation). The estimated

effective rate of deacclimation at 22°C at any point in chilling accumulation is thus

$$k_{deac_{22^\circ C}}^*(species, chill) = \max k_{deac_{22^\circ C}}(species) \times \Psi_{deacc}(chill), \quad [2]$$

where the effective rate of deacclimation  $k_{deac_{22^\circ C}}^*$  is a function of species and chill accumulation through its two components:  $\max k_{deac_{22^\circ C}}$  being a function of species and  $\Psi_{deacc}$ , which is a function of chill accumulation.

Using deacclimation potential as the metric for dormancy progression, all of the species examined respond similarly to chilling exposure (Fig. 6A and SI Appendix, Fig. S13), despite very different field phenology. The inflection point  $c$  of the deacclimation potential sigmoid curves, representing the amount of chilling needed for ~50% of maximum deacclimation rates, varied between 52 and 76 chill portions for all 15 species (Fig. 6B). In comparison, the standard determination of chilling requirement based on budbreak (here, chill required for 50% budbreak within 15 d was used) (dashed lines in Fig. 3) produced values ranging from 37 to 96 chill portions (Fig. 6B). Using this historical metric, *Forsythia* × ‘Meadowlark’ would be considered to have a low chill requirement (37 portions) and become ecodormant in early winter in the location of this study, whereas *A. balsamea* would be considered a high-chill requirement species (96 chill portions) and would not reach ecodormancy until the beginning of spring. The chill requirement based on 15 d to budbreak is highly negatively correlated with the  $\max k_{deac_{22^\circ C}}$  ( $r = -0.78$ ) (SI Appendix, Fig. S14A). This means that as chill accumulates over the progression of winter, species with faster maximum rates will reach the rate necessary to lose cold hardness and break bud within 15 d at lower chill accumulation than those with slower maximum rates. However, deacclimation rates continue to increase in response to chilling.

#### Effect of Temperature on Rates of Deacclimation (Forcing).

To evaluate how temperatures affect the rates of deacclimation, buds were collected from 13 of the 15 species at 54 and 82 portions of chill accumulation (not all 13 were collected at both times). These buds were deacclimated at seven temperatures between 2°C and 30°C. As expected, lower temperatures result

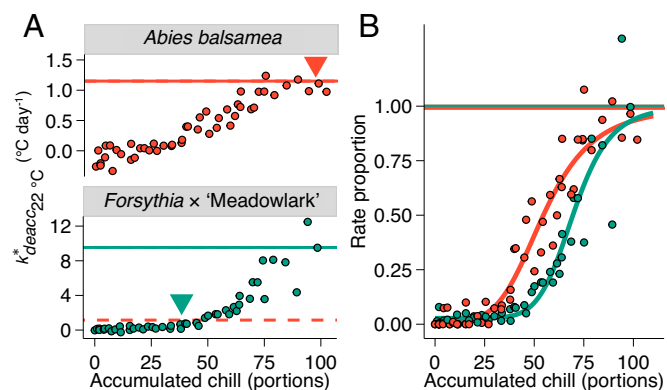


**Fig. 5.** Increase in deacclimation rates in response to chill accumulation. (A) Rates of deacclimation increased with chill accumulation. Full lines show maximum rates of deacclimation at 22°C as the average of the four highest deacclimation rates for each species. The dashed red line shows the maximum rate for *A. balsamea* within the *Forsythia* × ‘Meadowlark’ plot for comparison. Arrowheads show chill accumulation for dormancy transition based on budbreak. When normalized to the maximum rate of deacclimation for each species, a normalized rate proportion is produced (B), showing a much similar progression of dormancy.

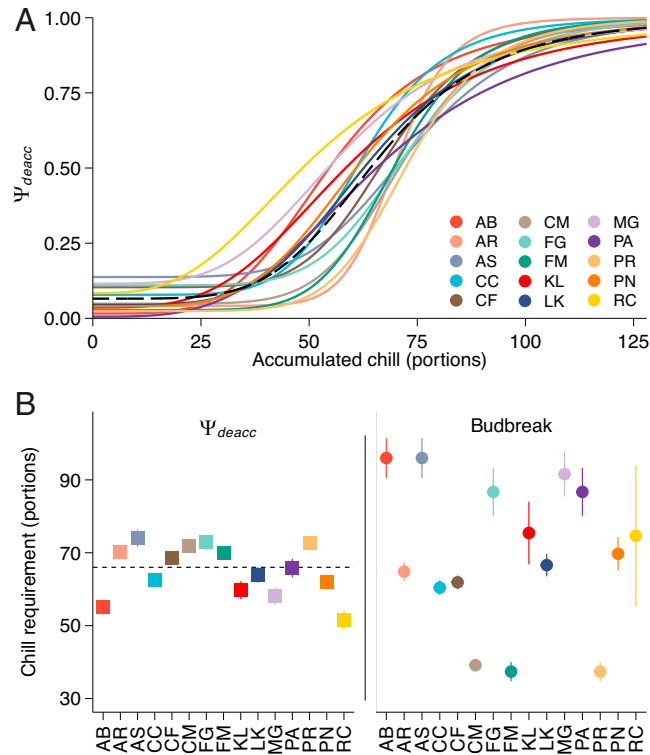


**Fig. 6.** Dormancy progression based on deacclimation rates and time to budbreak. (A) Normalized rates of deacclimation produce the deacclimation potential for all species ( $51 \geq n \geq 49$ ). (B) Inflection points of the deacclimation potential (the  $c$  term from Eq. 6 and *Materials and Methods*; curves in A) are similar across species, unlike chill requirement based on budbreak. Dashed lines (A and B) show the average based on the deacclimation potential of all 15 species studied. Error bars, when visible, represent SD. AB, *A. balsamea*; AR, *A. rubrum*; AS, *A. saccharum*; CC, *C. canadensis*; CF, *C. florida*; CM, *C. mas*; FG, *F. grandifolia*; FM, *Forsythia* × ‘Meadowlark’; KL, *K. latifolia*; LK, *L. kaempferi*; MG, *M. glyptostroboides*; PA, *P. abies*; PN, *P. nigra*; PR, *P. armeniaca*; RC, *R. calendulaceum*.

in slower deacclimation as compared with higher temperatures (Fig. 4B). The slopes for each temperature were extracted as deacclimation rates ( $k_{deaccT}^*$ , the effective rate of deacclimation at temperature  $T$ ) using a linear model (adjusted  $r^2 = 0.66$ ,  $F_{287,7384} = 53.9$ ,  $P < 0.001$  for all temperatures and species combined [individual fits are provided in *SI Appendix*]). Because these data refer to chilling accumulations of 54 and 82 portions where  $\Psi_{deacc} < 1$ , the values were normalized based on the rates measured at 22°C at each of these collections and the  $\max k_{deacc22^\circ\text{C}}$  for each species in order to isolate the effect of temperature. This correction transforms values of the measured, effective rates of deacclimation at a given temperature  $T$  ( $k_{deaccT}^*$ ) below maximum chill accumulation ( $\Psi_{deacc} < 1$ ) into the maximum possible rate at that temperature ( $\max k_{deaccT}$ ) based on Eq. 2. The effective rate of deacclimation at any temperature and chill accumulation thus becomes

$$k_{deaccT}^*(\text{species}, T, \text{chill}) = \max k_{deaccT}(\text{species}, T) \times \Psi_{deacc}(\text{chill}), \quad [3]$$

where the effective rate of deacclimation at temperature  $T$  is a function of species and temperature (through  $\max k_{deaccT}$ ) and chill accumulated (through  $\Psi_{deacc}$ ).

These corrected rates (i.e.,  $\max k_{deaccT}$ , where the effect of chill is removed) were then used to examine the response of rates of deacclimation to temperature (Fig. 7 and *SI Appendix*, Fig. S15). While a linear model produces a good fit for  $\max k_{deaccT}$  as a function of temperature (adjusted  $r^2 = 0.95$ ,  $F_{25,89} = 87.8$ ,  $P < 0.001$  for the 13 species combined), it is clear that the response to temperature increases faster at lower temperatures and tapers off at warmer temperatures of the

interval tested here for some species (e.g., *Forsythia* × ‘Meadowlark’ in Fig. 7). Therefore, a polynomial of the third order with intercept = 0 to allow for these curvatures was used.

Yet, despite accounting for the effects of forcing temperature and prior chilling on the rate of cold hardiness loss, differences in time to budbreak between species can still arise from how much cold hardiness a bud must lose for budbreak to occur (Eq. 1 and Fig. 1).

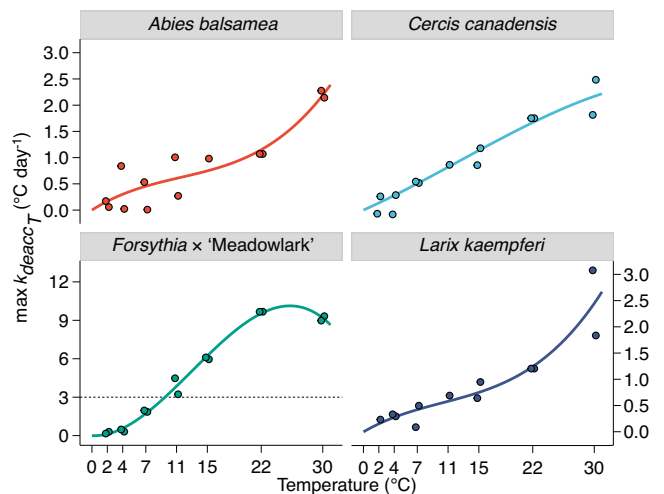


**Fig. 7.** Deacclimation rates in response to temperature. Deacclimation rates increase with increasing temperatures for all species ( $n = 14$ ). A different scale was used for *Forsythia* × ‘Meadowlark,’ but the dashed line shows the maximum value of scale for other species.

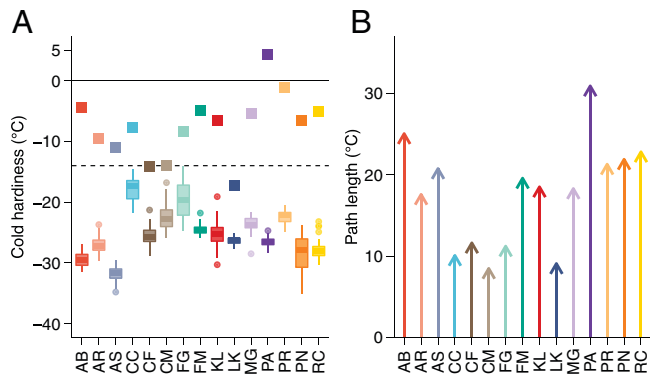


**Fig. 8.** Cold hardness parameters for each species. (A) Maximum cold hardness ( $CH_{max}$ ) observed in the 2019 to 2020 season (box plots;  $n = 10$ ) and cold hardness at budbreak ( $CH_{BB}$ ; squares) for each species (the dashed line shows the minimum temperature observed in the season for an idea of safety margins). (B) Path length ( $|CH_{max} - CH_{BB}|$ ) to budbreak for each species. AB, *A. balsamea*; AR, *A. rubrum*; AS, *A. saccharum*; CC, *C. canadensis*; CF, *C. florida*; CM, *C. mas*; FG, *F. grandifolia*; FM, *Forsythia* × 'Meadowlark'; KL, *K. latifolia*; LK, *L. kaempferi*; MG, *M. glyptostroboides*; PA, *P. abies*; PN, *P. nigra*; PR, *P. armeniaca*; RC, *R. calendulaceum*.

**Effect of Cold Hardness (Path Length).** To obtain the path length from a cold hardy state to budbreak for each species in field conditions, two measurements are required: the maximum field cold hardness ( $CH_{max}$ ; used in lieu of  $CH_0$ ) and the cold hardness at budbreak ( $CH_{BB}$ ) (Fig. 1).  $CH_{max}$  was obtained by averaging the cold hardness at the four time points during the winter where cold hardness in the field was maximum for each species (Fig. 8A).

To estimate  $CH_{BB}$ , the deacclimation curve was projected from initial cold hardness to the time of observed budbreak separately for each collection at 22 °C (where budbreak was measured) and averaged (SI Appendix, SI Text and Fig. S1).  $CH_{BB}$  values ranged from −17 °C to 4 °C (Fig. 8A). With values of  $CH_{BB}$  and  $CH_{max}$  determined, the path length is thus obtained as  $|CH_{max} - CH_{BB}|$ , and values ranged from 8 °C to 31 °C (Fig. 8B). Note that although *L. kaempferi* buds are about 10 °C more cold hardy than *C. canadensis*, the two species have very similar path lengths to budbreak because of different cold hardness at budbreak. In comparison, *L. kaempferi* and *Picea abies* buds have similar maximum cold hardness but differ in their  $CH_{BB}$ , thus resulting in different path lengths.

**Combining Effects of Chilling, Temperature, and Path Length Can Predict Field Budbreak.** Individual correlations of  $CH_{max}$ ,  $CH_{BB}$ , path length, and  $\max k_{deaccT}$  with timing of field budbreak are relatively poor, varying between  $r = -0.6$  and  $r = 0.5$  (SI Appendix Fig. S14 B–E). However, if a time to budbreak is calculated based on Eq. 1 (i.e., path length/ $\max k_{deaccT}$ ), this correlation increases to  $r = 0.88$  (SI Appendix, Fig. S14F), indicating that cold hardness parameters are good descriptors of field budbreak.

The dynamic cold hardness state in every winter is driven by the balance between the forces of acclimation and deacclimation during the dormant season (Fig. 3), and thus, it can set variable path lengths to budbreak at any moment during the season. In the fall, there is effectively very little, if any, deacclimation ( $k_{deaccT} \cong 0$ ) because although warm temperatures are still present ( $\max k_{deaccT} \gg 0$ ), chill accumulation is very low ( $\Psi_{deacc} \cong 0$ ) (Eq. 3). As chill accumulates during the winter, the potential for deacclimation increases ( $\Psi_{deacc} > 0$ ). However, winter temperatures are generally too low for significant levels of cold hardness loss to occur ( $\max k_{deaccT} \cong 0 \therefore k_{deaccT} \cong 0$ ). Once conditions begin to shift at the end of the dormant

season, both deacclimation potential is high ( $\Psi_{deacc} > 0$ ) and warmer spring temperatures occur ( $\max k_{deaccT} > 0$ ), thus resulting in net deacclimation ( $k_{deaccT}^* > 0$ ). Based on this framework, field cold hardness can be described as

$$CH_{field} = CH_{summer} + \int_{Fall}^{Spring} Acclimation dt + \int_{Fall}^{Spring} \max k_{deaccT} \times \Psi_{deacc} dt, \quad [4]$$

where  $CH_{summer}$  is the cold hardness of buds as they form in the late summer and fall, likely a function of species or genotype; *Acclimation* is a function of temperature where generally low temperatures promote greater gains in cold hardness but not part of this study; and  $\max k_{deaccT} \times \Psi_{deacc}$  describes any deacclimation occurring. Both acclimation and deacclimation portions are functions of temperature, but outdoor temperatures are a function of time; therefore, they are integrated over time ( $t$ ). Through these relationships, cold hardness throughout the winter can be predicted. In the fall, acclimation predominates, leading to gains in cold hardness; in the spring, deacclimation predominates, leading to loss of cold hardness. Additionally, field budbreak is predicted to occur in the spring once  $CH_{field} = CH_{BB}$ , therefore connecting the dormant and growing seasons.

To test whether prediction of field budbreak was possible, the time to run the path from maximum cold hardness in the field until the cold hardness at budbreak was predicted using only the temperature and chill relations established in growth chamber experiments, without optimization procedures. For this,  $CH_{max}$  and  $CH_{BB}$  were used for each species and their growth chamber-determined forcing ( $\max k_{deaccT}$ ) and chilling ( $\Psi_{deacc}$ ) responses. In addition, a set acclimation rate ( $k_{acc}$ ) was used for all species (limited to not increase observed  $CH_{max}$ ) (Materials and Methods). Therefore, cold hardness in the field is described here as

$$CH_{field} = CH_{max} + \int_{Fall}^{Spring} k_{acc} dt + \int_{Fall}^{Spring} \max k_{deaccT} \times \Psi_{deacc} dt, \quad [5]$$

where the trajectory predicted was only that of the loss of cold hardness in the spring, allowing for reacclimation, and the predicted day of field budbreak occurred when  $CH_{field} = CH_{BB}$ . In this way, Eq. 5 predicts the path of cold hardness loss in late winter and spring, and based on this information, the date when budbreak happens can be inferred (Fig. 9, Inset and SI Appendix, Fig. S16).

The resulting relationship between predicted (using Eq. 5) and observed budbreak for all 15 species used in this study combined is  $BB_{pred} = 1.98 + 1.01 \times BB_{observed}$  (Fig. 9) (adjusted  $r^2 = 0.91$ ,  $F_{1,13} = 148.1$ ,  $P < 0.001$ ), where  $BB_{observed}$  is the day of 50% budbreak in the field. It is important to note that 1) the only field-estimated parameter is  $CH_{max}$  2) there was no optimization of parameters obtained from growth chamber experiments (no training of the model), 3) the same acclimation rate was used for all species, and therefore, 4) the only input used for the model is the hourly temperature (and chilling calculated from it). In addition, this model also predicts the cold hardness of buds during the spring, which may be important to identify damage prior to budbreak in the field.

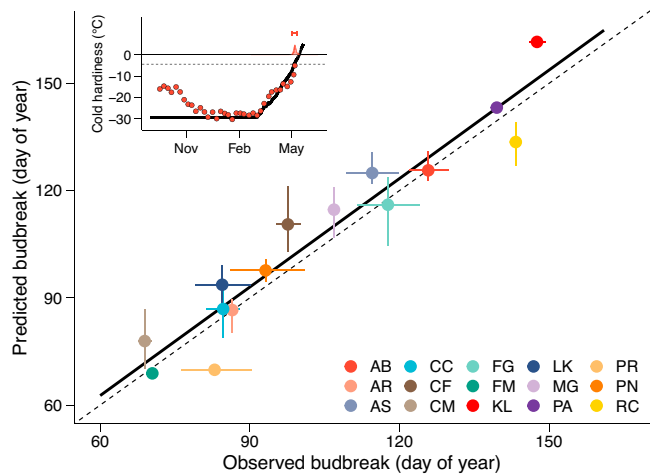


**Fig. 9.** Evaluation of budbreak predictions based on cold hardiness dynamics. Relationship between observed and predicted budbreak based on deacclimation dynamics. The dashed line represents a 1:1 relationship; the full line shows the calculated relationship:  $BB_{predicted} = 1.98 + 1.01 \times BB_{observed}$ , adjusted  $r^2 = 0.91$ ,  $P < 0.001$ . Horizontal error bars are the distribution of field budbreak from 5 to 95%; vertical error bars are the estimated error of prediction based on changes in initial cold hardiness ( $CH_{max} \pm 2.5^\circ\text{C}$ ). *Inset* shows an example for *A. balsamea* for how budbreak is predicted. Predicted cold hardiness (black line) starts at maximum cold hardiness ( $CH_{max}$ ), and budbreak is predicted (horizontal bar) when the cold hardiness prediction line crosses cold hardiness at budbreak ( $CH_{BBI}$ ; dashed line); circles show average measured cold hardiness, and the density plot at  $0^\circ\text{C}$  shows observed field budbreak. AB, *A. balsamea*; AR, *A. rubrum*; AS, *A. saccharum*; CC, *C. canadensis*; CF, *C. florida*; CM, *C. mas*; FG, *F. grandifolia*; FM, *Forsythia* × *Meadowlark*; KL, *L. latifolia*; LK, *L. kaempferi*; MG, *M. glyptostroboides*; PA, *P. abies*; PN, *P. nigra*; PR, *P. armeniaca*; RC, *R. calendulaceum*.

## Discussion

As the world becomes progressively warmer, spring phenology has continued to advance in time. However, the pace of advance in time to budbreak appears to be decreasing. Climate warming has led to shifts in chill accumulation (12, 28), where decreases in chill have been speculated to counterbalance increasingly warmer springs (28, 33, 64, 65). An effect that is largely ignored, however, is that warmer winter temperatures can also lead to less cold hardy buds. Here, changes in cold hardiness are demonstrated to affect the path to budbreak and thus, are an important but neglected dimension of spring phenology. Most importantly, through the investigation of cold hardiness dynamics, progression of dormancy is shown to be very similar across a wide range of diverse woody perennial species spanning the seed plant phylogeny. This suggests that classifications of low or high chill requirement are based mostly on forcing response, failing to describe physiological differences in dormancy.

**Acknowledging Cold Hardiness in Phenological Models.** This study uses aspects of cold hardiness dynamics to make inferences about budbreak phenology. This demonstrates the existence of a phenotype that is measured easily (although requiring some instrumentation) and much more so than determination of internal development of buds (e.g., refs. 66 and 67) and that can be measured prior to any external development in budbreak progression. In addition, cold hardiness dynamics clearly demonstrate the negative relationship between chilling and forcing (as plasticity) (15, 17, 33), indicating that this is not a measurement artifact (2).

Here, phenological plasticity is demonstrated by the  $\max k_{deacc_T} \times \Psi_{deacc}$  interaction (*SI Appendix*, Fig. S17). As a result, throughout the winter, growing degree day-like

accumulation changes; the same temperature has its effect modulated by how much chill has accumulated at any point in winter. This has previously been reported in deacclimation rates for *Cornus sericeae* (68) and several grapevine species (47), although with much less detail. On typical GDD-based models, this modulation by chilling is not dynamic; chill accumulation at a certain date is used to dictate the coefficient multiplying GDDs. However, an additional contribution to phenological plasticity can be explained from the cold hardiness viewpoint. Because cold hardiness must be lost through deacclimation to reach budbreak, typical models would account for this through accumulation of GDDs in a unidirectional manner. However, reacclimation can and often occurs especially in late winter and early spring (69), which would require negative GDDs. This is possible from a modeling standpoint but would be wrong if only based on the unidirectional concept of growth. Therefore, by understanding the basis for budbreak from the cold hardiness standpoint, for which positive and negative increments are possible, physiologically accurate concepts and models can be created that allow for these negative steps.

Based on the inclusion of cold hardiness modeling in plasticity of plant responses, some inferences can be made about how timing of budbreak can change. Previously reported variations in budbreak timing and chill requirement for the same species (especially if same genotype) in different latitudes or different climates (15, 17, 20, 70) can arise from two factors: the cold hardiness that is reached at any given location (depending largely on the lowest temperatures experienced) (71) (*SI Appendix*, Figs. S4 and S9) and differences in chill accumulation (12). Alternatively, when different genotypes are compared within the same environment (1, 15), differences in time to budbreak can arise from different levels of cold hardiness or different rates of deacclimation. In warming experiments (10, 13), higher temperature may lead to an expected higher rate of deacclimation (i.e., higher  $T$  for  $\max k_{deacc_T}$  in Eqs. 4 and 5) in response temperature and a lower cold hardiness during the dormant season (smaller path length) due to less acclimation, but this may be somewhat balanced by lower chill accumulation (lower  $\Psi_{deacc}$  in Eqs. 4 and 5; *SI Appendix*, *SI Text*).

While a phenology prediction model is inferred, the objective of this work was to define cold hardiness dynamics parameters for multiple species and to demonstrate how these are key to link the dormant and growing seasons. Therefore, no quantitative comparisons are made with other phenological models. In addition, the equations used here are only suggested fits for the measured experimental data rather than arbitrary expectations of what responses should be. Other models are available for prediction of cold hardiness, but those use different sets of estimates for endo- and ecodormancy phases and are mostly based on measurements of field cold hardiness or on a few experimental determinations of temperature effects (68, 72–77). Here, no assumptions regarding the qualitative phase of bud dormancy were made. Instead, exhaustive measurement of how cold hardiness is lost through weekly determinations during two dormant seasons are used to show a quantitative progression of dormancy (i.e., deacclimation potential— $\Psi_{deacc}$ ) rather than a simple division into endo- and ecodormancy phases.

Nonetheless, the parameters obtained in this study for temperature and chill responses resulted in good prediction of budbreak in the field in a single year of observation (Fig. 9). The robustness of this empirically based and yet, relatively simple model is demonstrated by an rms error of 7.5 d for 15 species, despite only four optimization iterations and only for

acclimation rate—for which a single rate was used for all species. Some error still arises from these parameters when compared with the cold hardiness path they predict (e.g., *C. canadensis* in *SI Appendix*, Fig. S16). However, knowledge of the shape of responses and general magnitude of the parameters examined in this study under controlled conditions makes it possible to optimize these to produce accurate field predictions for both cold hardiness and budbreak (i.e., training of the model). While it is clear that cold hardiness and deacclimation describe two critical components needed to resolve and predict budbreak, other environmental and biological attributes likely influence the precision of these estimates. For example, the actual temperature experienced by buds in the field is different from that of air temperature. At night, radiative cooling can decrease bud temperature below that of air; during the day, solar radiation may increase temperature, while wind may work to keep buds in equilibrium with air (41, 78, 79). Effects of radiation on bud temperature may be especially relevant for studies comparing species with buds several orders of magnitude difference in size, as in the present case.

**Considerations on Forcing.** Linear responses to temperature for phenological responses have been widely used in the literature ever since the concept of growing degree days was invented in the eighteenth century (80). Here, the curvature in the response of the rate of deacclimation to temperature results in residuals that are similarly skewed for most species if a linear relationship is used (as is generally the case); rates are underestimated at low temperatures and overestimated at moderate temperatures (*SI Appendix*, Fig. S18). It should be noted that previous works have modeled this nonlinear response (here as a polynomial of third degree) as a combination of an exponential and a logarithmic (47) or as a logistic response (2).

Nonlinearity of the forcing response has recently been suggested as a source of error in studies of spring phenology (81). Based on the relationship described here in Eq. 1, deacclimation rates are a relative measurement of thermal sensitivity (2, 20, 70, 71, 82). Observations of declines in thermal sensitivity (65) could, therefore, be arising from the seemingly exponential increase in deacclimation rate responses to low temperatures, leading into a linear phase of temperature response. The nonlinearity of response to temperature in deacclimation appears most clearly in some genotypes (e.g., *Forsythia* × 'Meadowlark') (Fig. 7). Measurements of deacclimation rates also show contributions toward growth of low but above freezing temperatures that would generally not be permitted to contribute to growing degree day calculations (below base temperature) (e.g., ref. 14). Here, those experiments were under a 0-h photoperiod, and it is likely that increased day length could further increase the contributions of these low temperatures (21, 39–44). The nonlinearity in response to temperature demonstrates that using only the change in temperature ( $\Delta T$ ) (15, 16, 71, 83) to predict future conditions may not be appropriate, although it is possible that temperature fluctuations around where responses are over- and underpredicted may result in good predictions.

The combination of differential cold hardiness in the field and diversity in rates of cold hardiness loss also results in uneven effects across species. The  $\max k_{deacc_{22^\circ C}}$  for *Forsythia* × 'Meadowlark' is  $9.5^\circ C d^{-1}$ , whereas it is  $0.6^\circ C d^{-1}$  for *R. calendulaceum*. This means that, in a warm winter, if all plants were  $6^\circ C$  less cold hardy than usual but still reached maximum chill accumulation, budbreak would change by less than a day for *Forsythia* × 'Meadowlark' ( $6^\circ C d^{-1}/9.5^\circ C d^{-1} = 0.63$  d) while decreasing by 10 d for *R. calendulaceum* at an air

temperature of  $22^\circ C$ . These effects are further exacerbated at common spring temperatures; the decrease in time to budbreak with  $6^\circ C$  less cold hardiness at an air temperature of  $7^\circ C$  would lead to only a 5-d decrease for *Forsythia* × 'Meadowlark' ( $\max k_{deacc_{7^\circ C}} = 1.17^\circ C d^{-1}$ ), while that decrease would be 25 d for *R. calendulaceum* ( $\max k_{deacc_{7^\circ C}} = 0.23^\circ C d^{-1}$ ). Therefore, although both species are responding to changes, their "responsiveness" measured by change in time to budbreak would be perceived as different (84).

**Including Cold Hardiness Can Improve Our Understanding of Chilling.** Chilling models are known to produce mixed results across regions. Here, the chill portions (dynamic) model (54, 55) was used for convenience and based on evidence of better transferability of findings across environments (85, 86). Furthermore, calculated chill portions and Utah chill units (52) have a correlation statistic higher than 0.995 in both years studied. However, many questions still remain regarding the temperatures at which chilling occurs and therefore, that contribute to advancing budbreak. Most chilling accumulation models do not account for chilling at below-freezing temperatures, but there is increasing evidence that they should (49, 50). It is possible that in some experiments, negative temperatures have led to increases in cold hardiness (e.g., refs. 22 and 45) and thus, longer paths to budbreak. Therefore, despite an increase in the rate of deacclimation (more chilling, greater  $\Psi_{deacc}$ , greater  $k_{deacc}^*$ ), the time to budbreak may not decrease. Even when negative temperatures are shown to contribute to chilling, it is possible that this effect is still underestimated because of these gains in cold hardiness.

Warm temperatures are also sometimes considered to contribute to chilling [e.g.,  $15^\circ C$  (21)]. In this case, their effects may be overestimated. While warmer temperatures may contribute to chill accumulation, they do promote greater loss of cold hardiness in buds than lower temperature (e.g.,  $11^\circ C$  vs.  $2^\circ C$  in Fig. 4B). Therefore, they decrease the path length to observe budbreak in these assays. Determining the cold hardiness as buds are removed from chilling chambers in these experiments can assign variation in time to budbreak to increased chilling vs. decreased path length in assays.

Different temperatures have also been shown to contribute differentially in terms of chilling across species (49, 50), which would suggest that models should be species specific. In contrast, evidence here is provided that the diverse species included in the study go through dormancy at a surprisingly similar pace (*SI Appendix*, Fig. S13). Temperature treatments imposed by Baumgarten et al. (50) may have had different effects in cold hardiness of each species during the chilling. Especially, below-freezing treatments may have promoted further acclimation of some species more than others, thus altering the path length and time to budbreak. This acclimation effect may have constituted the source of interspecific variation observed or at least contributed to it. Alternatively, variations in temperature in the field around optimum temperatures for each species may have resulted in homogeneous chilling for all species studied in the present work.

Considering all three scenarios (chilling by negative temperatures, chilling by warm temperatures, and different effects across species), it is clear that coupling cold hardiness measurements of buds with chilling assays can help parse out error in models resulting in nontranslatable results across regions. This demonstrates the necessity for more empirical studies of dormancy (11) combining cold hardiness with phenology. Future experiments assessing effects of chilling treatments on cold hardiness in controlled environments or determining the extent of



cold hardiness in different environments will help elucidate differences in chilling requirements observed across regions and years for the same species and even genotypes within species.

**Implications of a Conserved Dormancy Progression.** The pace in our understanding of plant dormancy has been very slow. The requirement of low temperatures to promote budbreak was first presented early in the nineteenth century (87). However, to this day experiments are being conducted to understand the contributions of temperatures to chilling in order to improve chill accumulation models. This is also true in terms of the molecular understanding of dormancy; the mechanism behind this important phenotype remains elusive (56, 57). Even the mechanism of chemicals known to help overcome dormancy and promote budbreak (i.e., hydrogen cyanamide) is yet to be described (58). It is possible that this is due to the fact that most studies compare species and genotypes with “low chill” and “high chill” requirement based on time to budbreak (e.g., refs. 59–61). The results presented here suggest that those chill requirements are mostly a result of a genotype’s response to forcing ( $r = -0.78$ ) and not different physiological stages of dormancy. Therefore, genes described in these studies as related to low or high chill phenotypes are potentially instead related to phenotypes of faster or slower growth (e.g., ref. 88).

The same dormancy progression for all plants posited in the present work does not change results seen in studies of local adaptation. Instead, the findings presented here provide empirical evidence that the response to temperature, or forcing, is more important than chilling in driving perceived differences in phenology across species within the same environment (2, 15, 23, 47, 70). Environments with low chilling accumulation tend to have warmer springs, and thus, the compensatory effects between chilling and forcing come into effect ( $\max k_{deacc}^{high\ T} \times \Psi_{deacc}^{low\ chill} \approx \max k_{deacc}^{low\ T} \times \Psi_{deacc}^{high\ chill}$ ) (SI Appendix, Fig. S17). Therefore, ambient spring temperatures and rates of deacclimation must be high enough to compensate for the lack of chill accumulation. However, if chilling is too low, budbreak may take too long even at high temperatures. This can be especially important for agricultural settings, where concentrated budbreak leading to synchronous flowering is important for management practices. However, as shown here, the absolute time to budbreak from these assays (compared with an arbitrary threshold) actually provides little information by itself in terms of the physiological stage of dormancy.

Several considerations can be made based on the sigmoid shape of the dormancy response, measured here in the form of  $\Psi_{deacc}$ . The effect of chilling is quantitative, and therefore, simply using qualitative determinations of endodormancy and ecodormancy (48) for buds cannot accurately describe the progression of dormancy. Although budbreak can and does occur at low chill accumulation, especially in those species with faster deacclimation rates, there is a critical state of chilling required before proper budbreak starts occurring (2). As an example, taking almost 100 d to break bud at 22 °C (earlier collections in Fig. 3 and SI Appendix, Fig. S10) would mean forfeiting most of the growing season (89). Locations with mild chill accumulation, such that they are in the linear portion of the  $\Psi_{deacc}$  sigmoid curve, will be most affected by climate warming, whereas regions with high chill accumulation (8) may take much longer before decreases in chilling produce sensible results; a decrease from 100 to 75 chill portions would decrease  $\Psi_{deacc}$  by 0.2, whereas a decrease from 75 to 50 chill portions reduces  $\Psi_{deacc}$  by 0.4 for the average of all species in this study,

resulting in uneven decreases in temperature sensitivity. Within a winter, this progression can lead to different increasing magnitudes in the effect of unseasonal midwinter warmings (winter weather whiplash) (90); the same amount of warming at 75 chill portions ( $\Psi_{deacc} = 0.68$ ) would cause more than double the deacclimation than at 50 chill portions ( $\Psi_{deacc} = 0.25$ ; this 25–chill portion difference was a 4- to 5-wk difference in time at the Arnold Arboretum in both years studied). Even if these warming events do not lead to budbreak ( $CH_{field} < CH_{BB}$ ) and potential spring frost damage (5), they could leave buds at risk for “invisible” midwinter damage should temperatures drop below cold hardiness of buds.

The same progression of dormancy for all plants observed here suggests two potential qualities for the molecular regulation of dormancy. One is that the chilling clock is an extremely conserved mechanism or an extreme case of convergent evolution (91); in the panel evaluated here, both gymnosperms and angiosperms, which diverged about 300 Mya, are represented and showed almost no difference in deacclimation potential in response to chilling (Fig. 6A). The second potential aspect is that the molecular mechanism is simple in the sense that little to no variation is possible within dormancy itself. There has been some evidence presented in this sense; single or few gene changes are able to completely disrupt dormancy from plants (92, 93), which is deleterious in temperate environments. Instead of variation in dormancy, the results presented here suggest that the timing of budbreak in plants is regulated only by differences in their cold hardiness and maximum rates of cold hardiness loss. This suggests evolution acting on these traits but not on the dormancy mechanism.

Contrary to the trend of studying plants in warmer environments, information for future adaptation was drawn here from how plants survive the cold. Using the cold hardiness dynamics phenotypes presented, clarity should arise from future studies of the relationships of dormancy and temperature but also, of other factors known to influence budbreak timing that were not included here (e.g., photoperiod, water availability, and wood porosity among others). It is clear that temperature affects three, and not only two, aspects related to dormancy: chilling, forcing, and cold hardiness. Plants in colder climates become more cold hardy (71) and therefore, have a longer path to budbreak than those in warmer climates. This status interacts with the level of chill accumulation reached prior to spring and the spring temperatures promoting forcing to result in budbreak. Using  $\Psi_{deacc}$  investigation of chilling models may yield better knowledge as to how temperatures contribute to chilling accumulation and dormancy transitions in plants and the overlapping temperature ranges of chilling and forcing (2). Considering the consistent dormancy progression across a wide range of species, contrasts between genotypes with low and high chilling requirements need to be reevaluated from a cold hardiness standpoint. Based on the findings presented here, these “different” chilling requirement phenotypes actually reflect inherently slower vs. faster deacclimation, less vs. more cold hardiness, or a combination of both. The framework suggested should be used to further investigate cold hardiness, chilling, and forcing responses of different plant species (47); genotypes within a species (1, 47); or even other taxa beyond plants (19, 82). However, awareness of a single woody plant response to chill accumulation should facilitate estimation of other parameters for modeling of spring phenology. Based on the broad range of species used, the impact of cold hardiness dynamics on phenology is likely universal across plants presenting cold season dormancy: a keystone phenotype defining the

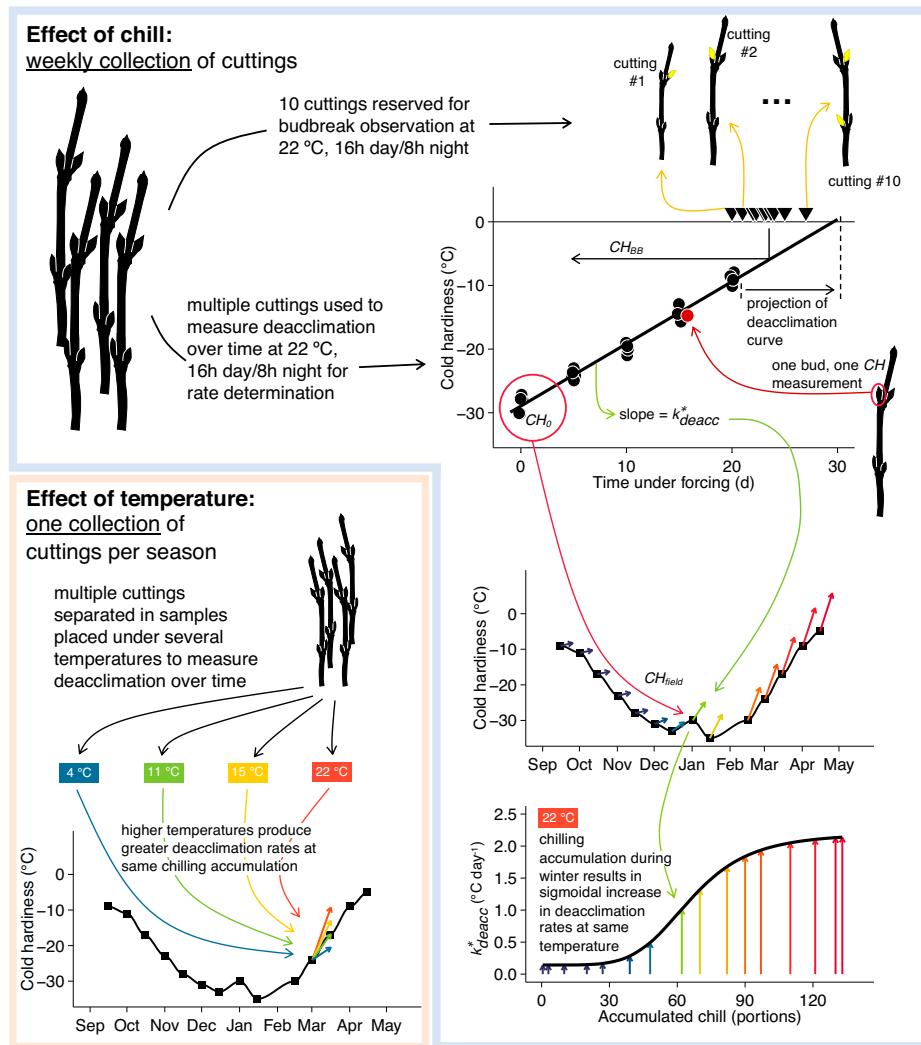


**Fig. 10.** Schematic representation of the methods used to determine cold hardiness dynamics parameters. Overall, sampling is separated between those used for the effect of accumulation of chill and the effect of temperature. In either case, cuttings are placed in cups of water to deacclimate within growth chambers, and cold hardiness is measured over time to determine deacclimation rates. For the effect of chill, weekly collections were performed and all deacclimated at 22°C. For the effect of temperature, one collection per season was performed, and cuttings were deacclimated at multiple temperatures (not all represented here).

dormant season that has been largely ignored but should be included in future studies.

## Materials and Methods

All material was collected from plants from the Arnold Arboretum of Harvard University located in Boston, MA (42°17'57"N, 71°07'22"W). The climate is a humid subtropical climate (Koeppen's Cfa) in US Department of Agriculture plant hardiness zone 6b [average annual extreme minimum temperature: -17.8°C to -15°C (94)]. Bud material was collected from 15 species: balsam fir (*A. balsamea*), red maple (*Acer rubrum*), sugar maple (*Acer saccharum*), Eastern redbud (*C. canadensis*), flowering dogwood (*Cornus florida*), cornelian cherry (*Cornus mas*), American beech (*Fagus grandifolia*), forsythia (*Forsythia* × 'Meadowlark'), mountain laurel (*Kalmia latifolia*), Japanese larch (*L. kaempferi*), dawn redwood (*Metasequoia glyptostroboides*), Norway spruce (*P. abies*), apricot (*Prunus armeniaca* 'Mikado'), Canadian plum (*Prunus nigra*), and flame azalea (*R. calendulaceum*). Cold hardiness of buds was evaluated using differential thermal analysis (95). Effect of chilling accumulation was evaluated in loss of cold hardiness (deacclimation) assays and time to budbreak assays, both under the same forcing conditions (22°C, 16-h day/8-h night). Deacclimation rates were normalized to maximum within species, resulting in deacclimation potential ( $\Psi_{deacc}$ ), which was modeled as a three-parameter log logistic:

$$\Psi_{deacc}(chill) = d + \frac{(1-d)}{1 + e^{b(\ln(chill) - \ln(c))}} \quad [6]$$

where the potential for deacclimation at the  $i$ th collection is a function of chilling accumulation at the  $i$ th collection. Three estimates are thus obtained:  $d$  is the minimum deacclimation observed at all times (analogous to an intercept);  $b$  is the slope associated with the log-logistic curve, where negative values indicate increases in  $\Psi_{deacc}$  as chill accumulation increases and greater magnitudes indicate a higher slope; and  $c$  is the inflection point of the log-logistic curve and therefore, a chilling requirement-analogous measurement as the chilling required to reach 50% of the maximum deacclimation rate. Effect of temperature was only evaluated in deacclimation assays. A graphic description of data collection is presented in Fig. 10. Detailed information for *Materials and Methods*, including all statistical analyses, is available in *SI Appendix, SI Materials and Methods*.

**Data Availability.** Cold hardiness measurements, time to budbreak measurements, and code for analyses have been deposited in GitHub ([https://github.com/apkovaleski/dormancy\\_ArnoldArb](https://github.com/apkovaleski/dormancy_ArnoldArb)) (96).

**ACKNOWLEDGMENTS.** I thank the Arnold Arboretum of Harvard University for access to the living collections; the Putnam Fellowship Program of the Arnold Arboretum for financial support; and R. L. Darnell, J. P. Londo, J. J. Grossman, F. E. Rockwell, the laboratory of A. J. Miller, I. L. Goldman, M. G. North, and F. J. Campos-Arguedas for comments on drafts.

1. E. Thibault, R. Soolanayakanahally, S. R. Keller, Latitudinal clines in bud flush phenology reflect genetic variation in chilling requirements in balsam poplar, *Populus balsamifera*. *Am. J. Bot.* **107**, 1597–1605 (2020).
2. I. Chuine, A unified model for budburst of trees. *J. Theor. Biol.* **207**, 337–347 (2000).
3. C. J. Chamberlain, B. I. Cook, I. Morales-Castilla, E. M. Wolkovich, Climate change reshapes the drivers of false spring risk across European trees. *New Phytol.* **229**, 323–334 (2021).
4. L. Gu *et al.*, The 2007 Eastern US spring freeze: Increased cold damage in a warming world? *BioScience* **58**, 253–262 (2008).
5. C. M. Zohner *et al.*, Late-spring frost risk between 1959 and 2017 decreased in North America but increased in Europe and Asia. *Proc. Natl. Acad. Sci. U.S.A.* **117**, 12192–12200 (2020).
6. C. K. Augspurger, Reconstructing patterns of temperature, phenology, and frost damage over 124 years: Spring damage risk is increasing. *Ecology* **94**, 41–50 (2013).
7. Y. Vitasse, L. Schneider, C. Rixen, D. Christen, M. Rebetez, Increase in the risk of exposure of forest and fruit trees to spring frosts at higher elevations in Switzerland over the last four decades. *Ag. For. Meteor.* **248**, 60–69 (2018).
8. Q. Liu *et al.*, Extension of the growing season increases vegetation exposure to frost. *Nat. Commun.* **9**, 426 (2018).
9. C. J. Chamberlain, B. I. Cook, I. García de Cortázar-Atauri, E. M. Wolkovich, Rethinking false spring risk. *Glob. Change Biol.* **25**, 2209–2220 (2019).
10. E. M. Wolkovich *et al.*, Warming experiments underpredict plant phenological responses to climate change. *Nature* **485**, 494–497 (2012).
11. H. Hänninen *et al.*, Experiments are necessary in process-based tree phenology modeling. *Trends Plant Sci.* **24**, 199–209 (2019).
12. E. Luedeling, E. H. Gitvet, M. A. Semenov, P. H. Brown, Climate change affects winter chill for temperate fruit and nut trees. *PLoS One* **6**, e20155 (2011).
13. A. D. Richardson *et al.*, Ecosystem warming extends vegetation activity but heightens vulnerability to cold temperatures. *Nature* **560**, 368–371 (2018).
14. R. A. Montgomery, K. E. Rice, A. Stefanski, R. L. Rich, P. B. Reich, Phenological responses of temperate and boreal trees to warming depend on ambient spring temperatures, leaf habit, and geographic range. *Proc. Natl. Acad. Sci. U.S.A.* **117**, 10397–10405 (2020).
15. A. K. Ettinger *et al.*, Winter temperatures predominate in spring phenological responses to warming. *Nat. Clim. Chang.* **10**, 1137–1142 (2020).
16. L. Meng *et al.*, Urban warming advances spring phenology but reduces the response of phenology to temperature in the conterminous United States. *Proc. Natl. Acad. Sci. U.S.A.* **117**, 4228–4233 (2020).
17. C. Bigler, Y. Vitasse, Daily maximum temperatures induce lagged effects on leaf unfolding in temperate woody species across large elevational gradients. *Front Plant Sci* **10**, 398 (2019).
18. T. F. Keenan, A. D. Richardson, K. Hufkens, On quantifying the apparent temperature sensitivity of plant phenology. *New Phytol.* **225**, 1033–1040 (2020).
19. D. N. Laskin *et al.*, Advances in phenology are conserved across scale in present and future climates. *Nat. Clim. Chang.* **9**, 419–425 (2019).
20. B. Wenden, M. Mariadassou, F.-M. Chmielewski, Y. Vitasse, Shifts in the temperature-sensitive periods for spring phenology in European beech and pedunculate oak clones across latitudes and over recent decades. *Glob. Change Biol.* **26**, 1808–1819 (2020).
21. D. F. B. Flynn, E. M. Wolkovich, Temperature and photoperiod drive spring phenology across all species in a temperate forest community. *New Phytol.* **219**, 1353–1362 (2018).
22. A. Lenz, G. Hoch, Y. Vitasse, C. Körner, European deciduous trees exhibit similar safety margins against damage by spring freeze events along elevational gradients. *New Phytol.* **200**, 1166–1175 (2013).
23. J. D. Fridley, Extended leaf phenology and the autumn niche in deciduous forest invasions. *Nature* **485**, 359–362 (2012).
24. M. D. Schwartz, R. Ahas, A. Aasa, Onset of spring starting earlier across the northern hemisphere. *Glob. Change Biol.* **12**, 343–351 (2006).
25. A. D. Richardson *et al.*, Climate change, phenology, and phenological control of vegetation feedbacks to the climate system. *Ag. For. Meteor.* **169**, 156–172 (2013).
26. A. Menzel, P. Fabian, Growing season extended in Europe. *Nature* **397**, 659 (1999).
27. T. F. Keenan *et al.*, Net carbon uptake has increased through warming-induced changes in temperate forest phenology. *Nat. Clim. Chang.* **4**, 598–604 (2014).
28. C. M. Zohner, L. Mo, T. A. M. Pugh, J.-F. Bastin, T. W. Crowther, Interactive climate factors restrict future increases in spring productivity of temperate and boreal trees. *Glob. Change Biol.* **26**, 4042–4055 (2020).
29. M. Chen, E. K. Melaas, J. M. Gray, M. A. Friedl, A. D. Richardson, A new seasonal-deciduous spring phenology submodel in the Community Land Model 4.5: Impacts on carbon and water cycling under future climate scenarios. *Glob. Change Biol.* **22**, 3675–3688 (2016).
30. T. F. Keenan, A. D. Richardson, The timing of autumn senescence is affected by the timing of spring phenology: Implications for predictive models. *Glob. Change Biol.* **21**, 2634–2641 (2015).
31. D. Zani, T. W. Crowther, L. Mo, S. S. Renner, C. M. Zohner, Increased growing-season productivity drives earlier autumn leaf senescence in temperate trees. *Science* **370**, 1066–1071 (2020).
32. Y. Vitasse, C. Signarbieux, Y. H. Fu, Global warming leads to more uniform spring phenology across elevations. *Proc. Natl. Acad. Sci. U.S.A.* **115**, 1004–1008 (2018).
33. H. Wang *et al.*, Overestimation of the effect of climatic warming on spring phenology due to misrepresentation of chilling. *Nat. Commun.* **11**, 4945 (2020).
34. Z. A. Panchen *et al.*, Leaf out times of temperate woody plants are related to phylogeny, deciduousness, growth habit and wood anatomy. *New Phytol.* **203**, 1208–1219 (2014).
35. S. Jochner *et al.*, Nutrient status: A missing factor in phenological and pollen research? *J. Exp. Bot.* **64**, 2081–2092 (2013).
36. O. L. Hajek, A. K. Knapp, Shifting seasonal patterns of water availability: Ecosystem responses to an unappreciated dimension of climate change. *New Phytol.* **233**, 119–125 (2022).
37. K. Shellie, A. P. Kovaleski, J. P. Londo, Water deficit severity during berry development alters timing of dormancy transitions in wine grape cultivar Malbec. *Sci. Hortic. (Amsterdam)* **232**, 226–230 (2018).
38. J. Laube, T. H. Sparks, N. Estrella, A. Menzel, Does humidity trigger tree phenology? Proposal for an air humidity based framework for bud development in spring. *New Phytol.* **202**, 350–355 (2014).
39. C. Körner, D. Basler, Plant science. Phenology under global warming. *Science* **327**, 1461–1462 (2010).
40. D. Basler, C. Körner, Photoperiod and temperature responses of bud swelling and bud burst in four temperate forest tree species. *Tree Physiol.* **34**, 377–388 (2014).
41. Y. Vitasse *et al.*, Impact of microclimatic conditions and resource availability on spring and autumn phenology of temperate tree seedlings. *New Phytol.* **232**, 537–550 (2021).
42. A. Erez, R. M. Samish, S. Lavee, The role of light in leaf and flower bud break of the peach (*Prunus persica*). *Physiol. Plant.* **19**, 650–659 (1966).
43. C. C. Brelsford, T. M. Robson, Blue light advances bud burst in branches of three deciduous tree species under short-day conditions. *Trees (Berl.)* **32**, 1157–1164 (2018).
44. C. Chiang *et al.*, Interactive effects of light quality during day extension and temperature on bud set, bud burst and *PaFTL2*, *PaCOL1-2*, and *PaSOC1* expression in Norway spruce (*Picea abies* (L.) Karst.). *Forests* **12**, 337 (2021).
45. A. Vitra, A. Lenz, Y. Vitasse, Frost hardening and dehardening potential in temperate trees from winter to budburst. *New Phytol.* **216**, 113–123 (2017).
46. J. P. Londo, A. P. Kovaleski, Characterization of wild North American grapevine cold hardiness using differential thermal analysis. *Am. J. Enol. Vitic.* **68**, 203–212 (2017).
47. A. P. Kovaleski, B. I. Reisch, J. P. Londo, Deacclimation kinetics as a quantitative phenotype for delineating the dormancy transition and thermal efficiency for budbreak in *Vitis* species. *AoB Plants* **10**, ply066 (2018).
48. G. A. Lang, J. D. Early, G. C. Martin, R. L. Darnell, Endo-, para-, and ecdormancy: Physiological terminology and classification for dormancy research. *HortScience* **22**, 371–377 (1987).
49. J. Cragin, M. Serpe, M. Keller, K. Shellie, Dormancy and cold hardiness transitions in winegrape cultivars Chardonnay and Cabernet Sauvignon. *Am. J. Enol. Vitic.* **68**, 195–202 (2017).
50. F. Baumgarten, C. M. Zohner, A. Gessler, Y. Vitasse, Chilled to be forced: The best dose to wake up buds from winter dormancy. *New Phytol.* **230**, 1366–1377 (2021).
51. J. Bennet, Temperature and bud rest period: Effect of temperature and exposure on the rest period of deciduous plant leaf buds investigated. *Calif. Agric.* **4**, 11–16 (1949).
52. E. A. Richardson, S. D. Seeley, D. R. Walker, A model for estimating the completion of rest for 'Redhaven' and 'Elberta' peach trees. *HortScience* **9**, 331–332 (1974).
53. A. D. Shaltout, C. R. Unrath, Rest completion prediction model for Starkrimson Delicious apples. *J. Am. Soc. Hortic. Sci.* **108**, 957–961 (1983).
54. S. Fishman, A. Erez, G. A. Couvillon, The temperature dependence of dormancy breaking in plants: Mathematical analysis of a two-step model involving a cooperative transition. *J. Theor. Biol.* **124**, 473–483 (1987).
55. S. Fishman, A. Erez, G. A. Couvillon, The temperature-dependence of dormancy breaking in plants: Computer-simulation of processes studied under controlled temperatures. *J. Theor. Biol.* **126**, 309–321 (1987).
56. J. E. K. Cooke, M. E. Eriksson, O. Junttila, The dynamic nature of bud dormancy in trees: Environmental control and molecular mechanisms. *Plant Cell Environ.* **35**, 1707–1728 (2012).
57. H. Yamane, A. K. Singh, J. E. K. Cooke, Plant dormancy research: From environmental control to molecular regulatory networks. *Tree Physiol.* **41**, 523–528 (2021).
58. I. A. Ionescu *et al.*, Transcriptome and metabolite changes during hydrogen cyanamide-induced floral bud break in sweet cherry. *Front Plant Sci* **8**, 1233 (2017).
59. Y. E. Miotto *et al.*, Spring is coming: Genetic analysis of the bud break date locus reveal candidate genes from the cold perception pathway to dormancy release in apple (*Malus x domestica* Borkh.). *Front Plant Sci* **10**, 33 (2019).
60. N. Vimont *et al.*, From bud formation to flowering: Transcriptomic state defines the cherry developmental phases of sweet cherry bud dormancy. *BMC Genomics* **20**, 974 (2019).
61. D. D. Porto *et al.*, Transcription profiling of the chilling requirement for bud break in apples: A putative role for *FLC-like* genes. *J. Exp. Bot.* **66**, 2659–2672 (2015).
62. Y. Vitasse, D. Basler, Is the use of cuttings a good proxy to explore phenological responses of temperate forests in warming and photoperiod experiments? *Tree Physiol.* **34**, 174–183 (2014).
63. G. Neuner, K. Monitzer, D. Kaplenig, J. Ingruber, Frost survival mechanism of vegetative buds in temperate trees: Deep supercooling and extraorgan freezing vs. ice tolerance. *Front Plant Sci* **10**, 537 (2019).
64. H. Yu, E. Luedeling, J. Xu, Winter and spring warming result in delayed spring phenology on the Tibetan Plateau. *Proc. Natl. Acad. Sci. U.S.A.* **107**, 22151–22156 (2010).
65. Y. H. Fu *et al.*, Declining global warming effects on the phenology of spring leaf unfolding. *Nature* **526**, 104–107 (2015).
66. A. Viherä-Aarnio, S. Sutinen, J. Partanen, R. Häkkinen, Internal development of vegetative buds of Norway spruce trees in relation to accumulated chilling and forcing temperatures. *Tree Physiol.* **34**, 547–556 (2014).
67. A. P. Kovaleski, J. P. Londo, K. D. Finkelstein, X-ray phase contrast imaging of *Vitis* spp. buds shows freezing pattern and correlation between volume and cold hardiness. *Sci. Rep.* **9**, 14949 (2019).
68. K. D. Kobayashi, L. H. Fuchigami, C. J. Weiser, Modeling cold hardiness of red-osier dogwood. *J. Am. Soc. Hortic. Sci.* **108**, 376–381 (1983).
69. S. R. Kalberer, N. Leyva-Estrada, S. L. Krebs, R. Arora, Frost dehardening and rehardening of floral buds of deciduous azaleas are influenced by genotypic biogeography. *Environ. Exp. Bot.* **59**, 264–275 (2007).
70. X. Geng *et al.*, Climate warming increases spring phenological differences among temperate trees. *Glob. Change Biol.* **26**, 5979–5987 (2020).
71. A. Lenz, G. Hoch, Y. Vitasse, Fast acclimation of freezing resistance suggests no influence of winter minimum temperature on the range limit of European beech. *Tree Physiol.* **36**, 490–501 (2016).
72. J. C. Ferguson, J. M. Tarara, L. J. Mills, G. G. Grove, M. Keller, Dynamic thermal time model of cold hardiness for dormant grapevine buds. *Ann. Bot.* **107**, 389–396 (2011).
73. J. C. Ferguson, M. M. Moyer, L. J. Mills, G. Hoogenboom, M. Keller, Modeling dormant bud cold hardiness and budbreak in twenty three *Vitis* genotypes reveals variation by region of origin. *Am. J. Enol. Vitic.* **65**, 59–71 (2014).
74. S. Kellomäki *et al.*, A simulation model for the succession of the boreal forest ecosystem. *Silva Fenn.* **26**, 1–18 (1992).
75. H. Hänninen, Climate warming and the risk of frost damage to boreal forest trees: Identification of critical ecophysiological traits. *Tree Physiol.* **26**, 889–898 (2006).
76. I. Leinonen, A simulation model for the annual frost hardiness and freeze damage of scots pine. *Ann. Bot.* **78**, 687–693 (1996).
77. I. Leinonen, R. Repo, H. Hänninen, K. E. Burr, A second-order dynamic model for the frost hardiness of trees. *Ann. Bot.* **76**, 89–95 (1995).
78. A. J. P. Quiñones, M. Keller, M. R. S. Gutierrez, L. Khot, G. Hoogenboom, Comparison between grapevine tissue temperature and air temperature. *Sci. Hortic. (Amsterdam)* **247**, 407–420 (2018).
79. J. Grace, The temperature of buds may be higher than you thought. *New Phytol.* **170**, 1–3 (2006).
80. M. Reaumur, Observations du thermometre, faites à Paris pendant l'année 1735, comparées avec celles qui ont été faites sous la ligne, à l'Isle de France, à Alger, & en quelques-unes de nos Isles de l'Amérique. *Mém. Acad. R. Sci. (Paris)* **1735**, 545–576 (1735).

81. E. M. Wolkovich *et al.*, A simple explanation for declining temperature sensitivity with warming. *Glob. Change Biol.* **27**, 4947–4949 (2021).
82. S. J. Thackeray *et al.*, Phenological sensitivity to climate across taxa and trophic levels. *Nature* **535**, 241–245 (2016).
83. W. Buermann *et al.*, Widespread seasonal compensation effects of spring warming on northern plant productivity. *Nature* **562**, 110–114 (2018).
84. C. Parmesan, Influences of species, latitudes and methodologies on estimates of phenological response to global warming. *Glob. Change Biol.* **13**, 1860–1872 (2007).
85. E. Luedeling, Climate change impacts on winter chill for temperate fruit and nut production: A review. *Sci. Hortic. (Amsterdam)* **144**, 218–229 (2012).
86. J. Zhang, C. Taylor, The dynamic model provides the best description of the chill process on 'Sirora' pistachio trees in Australia. *HortScience* **46**, 420–425 (2011).
87. T. A. Knight, XV. Account of some experiments on the ascent of the sap in trees. In a letter from Thomas Andrew Knight, Esq. to the Right Hn. Sir Joseph Banks, Bart. K. B. P. R. S. *Philos. Trans. R. Soc. Lond.* **91**, 333–353 (1801).
88. A. P. Kovaleski, J. P. Londo, Tempo of gene regulation in wild and cultivated *Vitis* species shows coordination between cold deacclimation and budbreak. *Plant Sci.* **287**, 110178 (2019).
89. C. M. Zohner, L. Mo, V. Sebold, S. S. Renner, Leaf-out in northern ecotypes of wide-ranging trees requires less spring warming, enhancing the risk of spring frost damage at cold range limits. *Glob. Ecol. Biogeogr.* **29**, 1065–1072 (2020).
90. N. J. Casson *et al.*, Winter weather whiplash: Impacts of meteorological events misaligned with natural and human systems in seasonally snow-covered regions. *Earths Futur.* **7**, 1434–1450 (2019).
91. S. Yeaman *et al.*, Convergent local adaptation to climate in distantly related conifers. *Science* **353**, 1431–1433 (2016).
92. S. Tylewicz *et al.*, Photoperiodic control of seasonal growth is mediated by ABA acting on cell-cell communication. *Science* **360**, 212–215 (2018).
93. D. G. Bielenberg *et al.*, A deletion affecting several gene candidates is present in the *Evergrowing* peach mutant. *J. Hered.* **95**, 436–444 (2004).
94. M. S. Dosmann, The history of minimum temperatures at the Arnold Arboretum: Variation in time and space. *Arnoldia* **72**, 2–11 (2015).
95. L. J. Mills, J. C. Ferguson, M. Keller, Cold-hardiness evaluation of grapevine buds and cane tissues. *Am. J. Enol. Vitic.* **57**, 194–200 (2006).
96. A. P. Kovaleski, Data from "Woody species do not differ in dormancy progression: Differences in time to budbreak due to forcing and cold hardiness." GitHub. [https://github.com/apkovaleski/dormancy\\_ArnoldArb](https://github.com/apkovaleski/dormancy_ArnoldArb). Deposited 14 April 2022.